Available online at www.sciencedirect.com
ScienceDirect
Medical Engineering & Physics 31 (2009) 287–294
Medical Engineering & Physics
www.elsevier.com/locate/medengphy

Parametric study on the interface pullout strength of the vertebral body replacement cage using FEM-based Taguchi methods

Wen-Hsien Hsu [a], Ching-Kong Chao [a], Hsi-Ching Hsu [b], Jinn Lin [b], Ching-Chi Hsu [a,*]

[a] Department of Mechanical Engineering, National Taiwan University of Science and Technology, Taipei 106, Taiwan, ROC
[b] Department of Orthopaedic Surgery, National Taiwan University Hospital, Taipei 100, Taiwan, ROC

Received 3 December 2007; received in revised form 27 June 2008; accepted 1 July 2008

Abstract

Improper design of vertebral body cages may seriously affect the interface strength and cause the lose of fixation for a vertebral body replacement. This research used a FEM-based Taguchi method to investigate the effects of various factors to find the robust design of the body cage. Three-dimensional finite element models with a nonlinear contact analysis have been developed to simulate the pullout strength of the body cage. Then, the Taguchi robust design method was used to evaluate the spike design. In a situation without bone fusion, the spike row, the spike oblique, and the spike height were especially important factors. The optimum combination has been found to be the pyramidal spike type, a spike height of 2 mm, a spike diameter of 2.2 mm, an oblique geometry, 11 rows per 28 mm, and an inner diameter of 10 mm. In a situation with bone fusion, the spike row, the spike height, and the inner diameter were the most significant factors. Here, the optimum combination has been found to be the conical spike type, a spike height of 2 mm, a spike diameter of 2.2 mm, an oblique geometry, 11 rows per 28 mm, and an inner diameter of 20 mm. The finite element analyses could be used to predict the interface stiffness of the body cages. The FEM-based Taguchi methods have effectively decreased the time and effort required for evaluating the design variables of implants and have fairly assessed the contribution of each design variable.

Keywords: Body cage; Pullout strength; Finite element analysis; Taguchi method

1. Introduction

Body cages have been used to treat vertebral bodies with different maladies such as severe compression fracture, dislocation, tumor, or infection [1–3]. However, a vertebral body replacement commonly experiences graft fracture, loosening, and collapse in a short period after an orthopaedic surgery. From the literature, subsidence of a body cage into the vertebral body may cause severe problems such as the collapse of the vertebral body, progression of kyphosis, or fusion failure [4,5]. Implant subsidence occurs frequently in patients with osteoporosis, where a lower bone mineral density is associated with lower bone strength [6–9]. Past research has focused mainly on the subsidence of the body cage but has neglected certain mechanical suitabilities. In clinical observations, the failure modes of a vertebral body replacement have been found to consist of not only implant subsidence but also interface loosening. Dietl et al. [10] tested three types of lumber interbody fusion cages to test the pullout performance. They concluded that the pullout resistance depended on the implant design. However, there is a wide variety of available body cage designs for lumbar vertebral body fusion surgery [11,12], and the effects of the design parameters have been unclear. In addition, there have been no studies that have addressed the effects of the design parameters of the body cage by using statistical engineering methods. Bone fusion is another consideration for lumbar vertebral body replacement. This factor could affect the load distribution on the vertebral body and the spine overall [13].

In this research, we suspected that the design of the body cage might also affect the bone fusion. To quantitatively identify these variables, the interface stiffness of the body cage

* Corresponding author at: Department of Mechanical Engineering, National Taiwan University of Science and Technology, No. 43, Section 4, Keelung Road, Taipei 106, Taiwan, ROC. Tel.: +886 2 27333141x7597; fax: +886 2 27376460.
E-mail address: mechi0924@yahoo.com.tw (C.-C. Hsu).

1350-4533/$ – see front matter © 2008 IPEM. Published by Elsevier Ltd. All rights reserved.
doi:10.1016/j.medengphy.2008.07.001

was obtained by using finite element models with a nonlinear contact analysis. Then, the Taguchi robust design method which has been applied for biomechanics studies [14–21] was used to calculate the contribution of each design parameter in order to find the optimal design parameters of the body cage. Two kinds of situations are here discussed: (1) with bone fusion and (2) without bone fusion. Finally, the mechanical tests were conducted to validate the applicability of the finite element models. The aims of this study were to assess the contribution of each design variable and to find the optimal combination of the body cage.

2. Materials and methods

2.1. Finite element analysis

Finite element analysis is a powerful tool to examine complex sample shapes with complicated loading and boundary conditions [22]. For this research, the three-dimensional finite element models which consisted of the body cage and both bone cuffs were created. The CAD program SolidWorks 2005 (SolidWorks Corporation, Concord, MA, USA) and the finite element software COSMOSworks 2005 (Structural Research and Analysis Corporation, Los Angeles, CA, USA) were used. Six design factors of the body cage were considered including the spike type (ST), the spike height (SH), the spike diameter (SD), the spike oblique (SO), the spike row (SR), and the inner diameter (ID) (Fig. 1). The body cage was 50 mm in height and 28 mm in outer diameter. Two bricks of bone cuffs (50 mm × 50 mm × 10 mm) were assumed to simulate the surrounding bones of a vertebral body with osteoporosis.

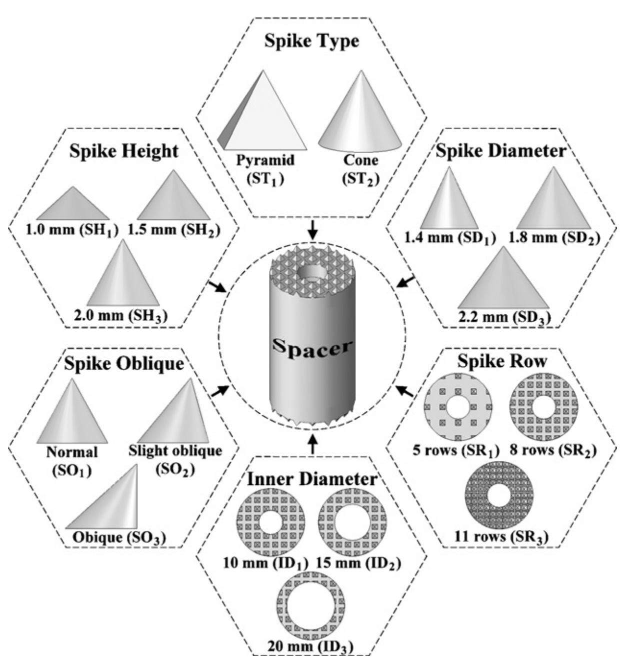

Fig. 1. Definition of design variables for the body cage.

A three-dimensional isotropic tetrahedral solid element was used for modeling the body cage and the bone cuffs. The body cage and the bone cuffs were free-meshed and the convergent analysis was done by resetting the element size controls. For the models without bone fusion, a total number of elements ranged from 46,000 to 209,000 and a total number of nodes ranged from 71,000 to 286,000. For the models with bone fusion, a total number of elements ranged from 38,000 to 289,000 and a total number of nodes ranged from 55,000 to 380,000. The elastic modulus of the body cage which was made from Ti6Al4V was 114 GPa. The bone cuffs were assumed to be homogenous with an elastic modulus of 137.5 MPa. The Poisson's ratio was 0.3 for both the body cage and the bone cuffs. The interfaces between the body cage and the bone cuffs were contact, with the penetrating spikes pointing in the direction of the body cage displacement. The coefficient of friction was set to zero. In the loading condition, a compressive force of 200 N was loaded on the end surface of both bone cuffs. In real life, the causes and conditions of pullout are complicated, but for the present study, we assumed that a displacement of 0.1 mm was applied to the surface of the body cage to simulate a pullout. The boundary conditions were constrained at the outer surfaces of the bone cuffs in the z-direction to simulate the body cage pullout from the bones (Fig. 2A).

In order to investigate the effects of bone fusion, two models, with and without bone fusion, were analyzed. In the situation with bone fusion, the elastic modulus of the fusion bone remained at 137.5 MPa. The fusion bone was inserted inside the body cage and the interface between the fusion bone and the adjacent vertebral bodies (the bone cuffs) was assumed to be a perfect bond. In the postprocessing analysis, the total reaction force was chosen to represent the bone adhesion to the body cage. The total reaction force was defined to be the summation of the nodal reaction force over the surface with a pre-applied displacement.

2.2. Factorial analysis by Taguchi robust design method

The Taguchi robust design method is a scientifically disciplined tool for conducting and evaluating improvements in materials, products, equipment, and processes [23]. The purposes of these improvements are to enhance the desired overall performance. Key process control parameters are also examined to reduce the number of manufacturing defects, and further contribute to design optimization. The Taguchi method used a fractional factorial design to replace a full factorial design. This can largely reduce the number of experimental runs. In this research, a higher total reaction force obtained from the finite element analysis represented better bone adhesion to the body cage. Therefore, the total reaction force was transformed into a the-larger-the-better signal-to-noise ratio, $S/N = -10 \log(1/y_i^2)$ where y_i is the result of the ith run.

Six control factors for the body cage were selected and discrete values for each factor were defined as follows: pyra-

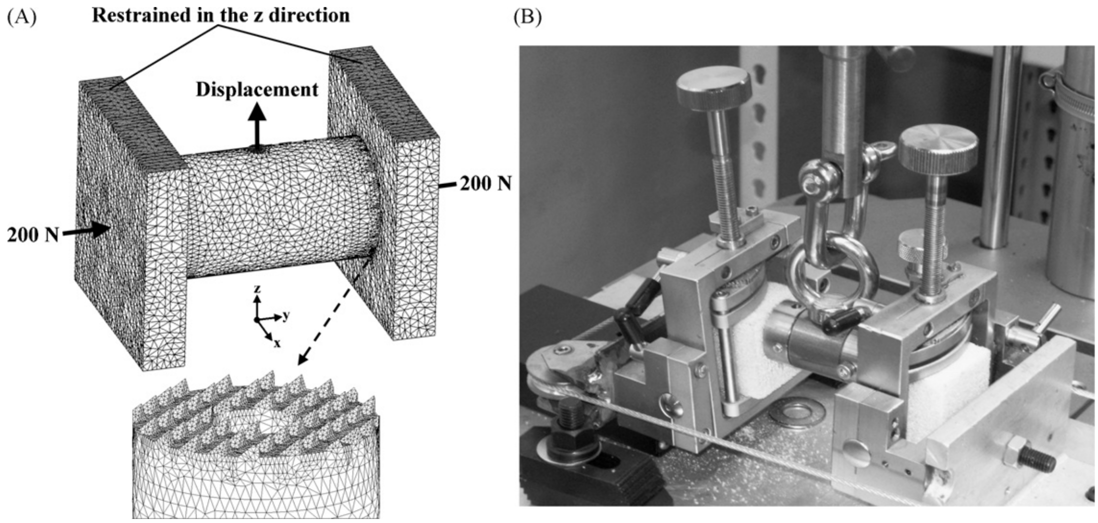

Fig. 2. (A) The boundary and loading condition of the finite element models and (B) the setup of the pullout tests.

mid or cone for the spike type; 1, 1.5, or 2 mm for the spike height; 1.4, 1.8, or 2.2 mm for the spike diameter; normal, slight oblique, or oblique for the spike oblique; 5, 8, or 11 rows per 28 mm for the spike row; 10, 15, or 20 mm for the inner diameter. The L_{18} orthogonal array, which could control one variable at two levels and seven variables at three levels, was used. Then the matrix experiments were conducted according to the arrangements of the L_{18} orthogonal array (Table 1). From the S/N ratio plots, the factor levels corresponding to the maximum S/N constituted the optimum variable-level combination of the body cage.

The significance of the design factor of the body cage was estimated by the analysis of variance (ANOVA) statistical method. An ANOVA table consists of the total sum of squares, the degrees of freedom, the mean square, the F value, and the weight of contribution. The equation for the total sum of squares, which measures the overall variability of the data, is $SS_T = \sum_{i=1}^{n}(S/N_i - \overline{S/N})^2$ where n is the number of runs, S/N_i the S/N of the ith run, and $\overline{S/N}$ is the overall mean of S/N. The equation for the sum of squares for the factors, which measures the variability due to the factors, was $SS_F = \sum_{i=1}^{m} N_{Fi}(\overline{S/N}_{Fi} - \overline{S/N})^2$ where F is the design factor from U to Z, m the number of discrete levels, N_{Fi} the number of runs at each level of each factor, and $\overline{S/N}_{Fi}$ is the mean of S/N at each level of each factor. SS_E, which measures the variability due to the error, can be calculated by subtracting SS_F from SS_T. The equation was $SS_E = SS_T - SS_U - SS_V - SS_W - SS_X - SS_Y - SS_Z$. There were 15 degrees of freedom in the L_{18} orthogonal array, and those of each factor were defined by subtracting 1 from the

Table 1
The L_{18} orthogonal array and the total reaction force obtained from finite element analysis

Run	Spike type	Spike height (mm)	Spike diameter (mm)	Spike oblique	Spike row (rows)	Inner diameter (mm)	Total reaction force (N)	
							Without bone fusion	With bone fusion
1	Pyramid	1	1.4	Normal	5	10	318.70	421.61
2	Pyramid	1	1.8	Slight oblique	8	15	400.53	449.81
3	Pyramid	1	2.2	Oblique	11	20	647.00	718.29
4	Pyramid	1.5	1.4	Normal	8	15	485.17	521.88
5	Pyramid	1.5	1.8	Slight oblique	11	20	582.70	611.21
6	Pyramid	1.5	2.2	Oblique	5	10	552.50	576.80
7	Pyramid	2	1.4	Slight oblique	5	20	429.22	609.74
8	Pyramid	2	1.8	Oblique	8	10	630.95	661.71
9	Pyramid	2	2.2	Normal	11	15	644.65	706.36
10	Cone	1	1.4	Oblique	11	15	563.23	634.83
11	Cone	1	1.8	Normal	5	20	218.24	531.13
12	Cone	1	2.2	Slight oblique	8	10	536.40	585.41
13	Cone	1.5	1.4	Slight oblique	11	10	619.96	667.20
14	Cone	1.5	1.8	Oblique	5	15	327.10	482.22
15	Cone	1.5	2.2	Normal	8	20	415.48	597.42
16	Cone	2	1.4	Oblique	8	20	553.11	671.09
17	Cone	2	1.8	Normal	11	10	563.02	660.59
18	Cone	2	2.2	Slight oblique	5	15	360.40	518.01

number of discrete levels ($m-1$). Mean square values were calculated by dividing the sum of square values for the factor and error by the respective degree of freedom. The mean square for the factor was $MS_F = SS_F/DOF_F$, where DOF_F is the degree of freedom for the respective factor. The mean square for the error was $MS_E = SS_E/DOF_E$, where DOF_E is the degree of freedom for the respective error. The F value for each factor was $F = MS_F/MS_E$, and the percentage contribution of each factor was $C = SS_F/SS_T \times 100\%$. Following the comparative study, it is necessary to conduct an experiment to verify the results relative to the required performance. Therefore, in this research, the verification experiment was performed using the optimum parameter level settings and it was evaluated by the additive model: $S/N_{add} = \overline{S/N} + \sum_{i=1}^{k}(\overline{S/N}_{OPTi} - \overline{S/N})$, where k is the number of design factors, and $\overline{S/N}_{OPTi}$ is the mean S/N of each design factor at the optimal level.

2.3. Mechanical experiments of pullout strength

Polyurethane foam (Pacific Research Lab., Vashon, WA, USA) with a density of 0.32 g/cm^3 was used in this study. Six types of the body cages, which were selected from the L_{18} orthogonal array, and one optimum design in the situation without bone fusion, which was obtained by Taguchi methods, were fabricated. The spike of the body cage was implanted into two bricks of the polyurethane foam bone. A compression force of 200 N which caused by a body weight was considered with use of a cable wire, pulleys, and counterweights. The body cages were pulled out from the foam bones at a loading rate of 5 mm/min (Fig. 2B). The load–displacement curves were recorded. One optimum design and six types of the body cages were repeated six times. The maximal force was defined as the pullout force.

3. Results

Eighteen FE models were constructed in accordance with the design variable combinations specified in the L_{18} orthogonal array table. The models with and without bone fusion were also discussed. Therefore, 36 finite element models were created in this study. The computational time ranged from 2 to 3 h for the models without bone fusion and from 2 to 4 h for the models with bone fusion. The convergence of the finite element models was achieved by resetting the element size controls. The body cages had negligible deformation because the osteoporotic bone was used (Fig. 3) and the reaction force was evenly distributed on the surface. The total reaction force of the finite element models was calculated and listed in Table 1. The total reaction force for the group of models with bone fusion increased to an average of 26% over those without bone fusion.

According to the results of the L_{18} orthogonal array (Table 1), the reaction force was transformed into a signal-to-noise ratio where a larger value is more desired. Then, the

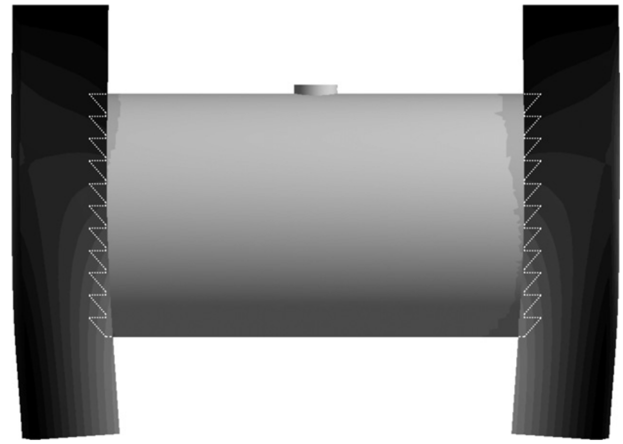

Fig. 3. The displacement distribution of the finite element models.

S/N ratio plots of the total reaction force at each level of every control variable were obtained (shown in Fig. 4A and B). The results in Fig. 4A (without bone fusion) suggested optimum factor level settings of $ST_1SH_3SD_3SO_3SR_3ID_1$, which correspond to the pyramidal spike type, a spike height of 2 mm, a spike diameter of 2.2 mm, an oblique geometry, 11 rows per 28 mm, and an inner diameter of 10 mm. The results in Fig. 4B (with bone fusion) suggested optimum factor level settings of $ST_2SH_3SD_3SO_3SR_3ID_3$, which correspond to the conical spike type, a spike height of 2 mm, a spike diameter of 2.2 mm, an oblique geometry, 11 rows per 28 mm, and an inner diameter of 20 mm.

The ANOVA tables (Tables 2 and 3) were obtained after performing a data analysis using the S/N ratios. From the

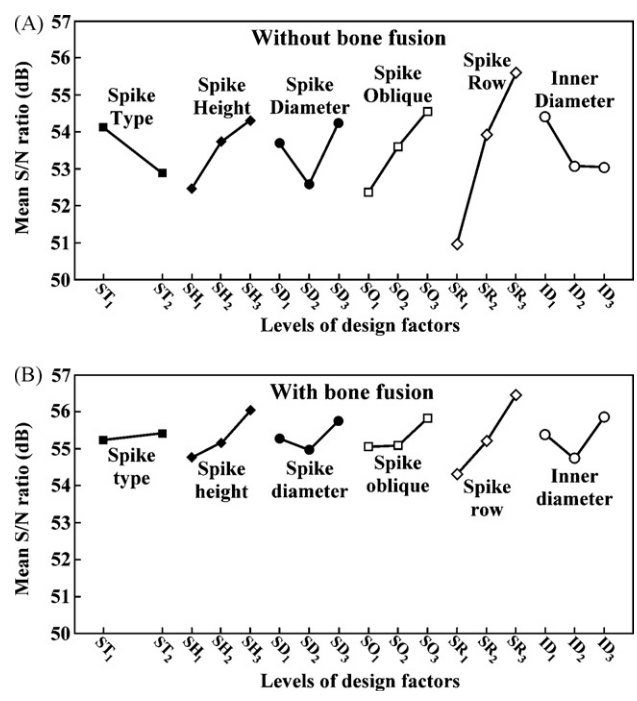

Fig. 4. S/N ratio plots of the total reaction force at each level of each design factor: (A) without bone fusion; (B) with bone fusion.

Table 2
ANOVA table for total reaction force in situation without bone fusion

Design factor	Sum of squares	Degrees of freedom	Mean square	F-Value	Contribution (%)
Spike type	6.91	1	3.46	5.14	5.96
Spike height	10.80	2	5.40	8.03	9.31
Spike diameter	8.52	2	4.26	6.33	7.34
Spike oblique	14.38	2	7.19	10.69	12.40
Spike row	66.14	2	33.07	49.16	57.01
Inner diameter	7.24	2	3.62	5.38	6.24
Error	2.02	4	0.67	–	1.74
Total	116.01	15	–	–	100

results of Table 2 (without bone fusion), the spike row density had the highest contribution (57.01%) to the pullout strength of the body cage. Following this, the descending order of contribution was the spike oblique (12.4%), spike height (9.31%), spike diameter (7.34%), inner diameter (6.24%), and spike type (5.96%). From the results of Table 3 (with bone fusion), the spike row density again had the highest contribution (45.69%), then the descending order of contribution was the spike height (17.06%), the inner diameter (12.44%), the spike oblique (7.65%), and the spike diameter (6.17%). The effect of the spike type was minimal (0.54%).

In the confirmation study (Table 4), for the situation without bone fusion, the results obtained from the finite element model were closely related to the additive model for both the initial design and the optimum design. The confirmation results indicated that the total reaction force of the optimum design was 763.20 N (57.65 db) higher than the initial design (318.70 N), and the S/N ratios increased by 7.58 db. In the situation with bone fusion, the results obtained from the finite element model were closely related to the additive model for both the initial design and the optimum design. The confirmation results showed that the total reaction force of the optimum design was 770.19 N (57.73 db) higher than the initial design (421.61 N), and the S/N ratios increased by 5.23 db.

In the mechanical tests, increasing the displacement of the body cage could increase the pullout force. The displacement was proportional to the pullout force before the peak force was reached. Then, the pullout force decreased when the foam bones were fractured (Fig. 5). The experimental results showed that the pullout force of the optimum body cage was significantly higher than that of six types of the body cages. The total reaction force was closely related to the pullout force with a high correlation coefficient of 0.802 (Fig. 6).

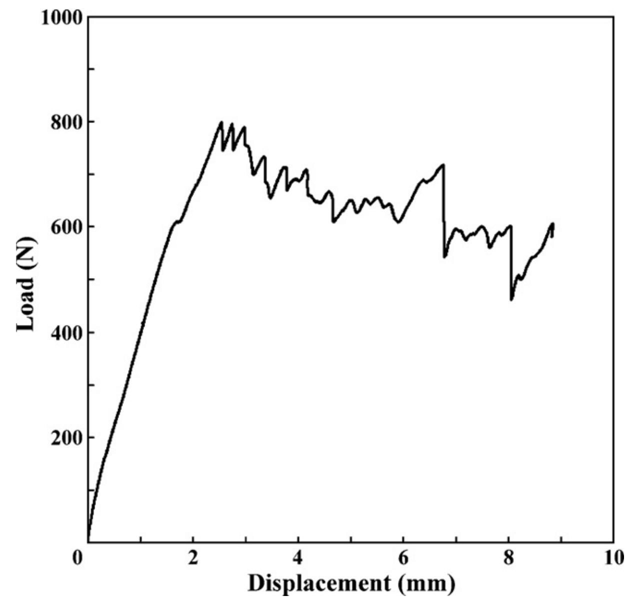

Fig. 5. The load–displacement curve of the body cage.

4. Discussion

In this study, we used FEM-based Taguchi methods to evaluate the pullout strength of the body cage and assess the effects of different spike designs. Referring to the past

Table 3
ANOVA table for total reaction force in situation with bone fusion

Design factor	Sum of squares	Degrees of freedom	Mean square	F-Value	Contribution (%)
Spike type	0.17	1	0.08	0.08	0.54
Spike height	5.22	2	2.61	2.45	17.06
Spike diameter	1.89	2	0.94	0.89	6.17
Spike oblique	2.34	2	1.17	1.10	7.65
Spike row	13.98	2	6.99	6.56	45.69
Inner diameter	3.81	2	1.90	1.79	12.44
Error	3.20	4	1.07	–	10.45
Total	30.59	15	–	–	100

Table 4
The results of verification experiments

	Initial design ($ST_1SH_1SD_1SO_1SR_1ID_1$)	Optimum design ($ST_1SH_3SD_3SO_3SR_3ID_1$)	Gain (db)
Without bone fusion			
Additive model (db)	50.49	59.69	9.20
Finite element model (db)	50.07	57.65	7.58
	Initial design ($ST_1SH_1SD_1SO_1SR_1ID_1$)	Optimum design ($ST_2SH_3SD_3SO_3SR_3ID_3$)	Gain (db)
With bone fusion			
Additive model (db)	53.38	58.74	5.36
Finite element model (db)	52.50	57.73	5.23

research about the body cage, the authors presented the results obtained from clinical observations and discussed the relationship between the implant design and its biomechanical performance. In a previous study, Fayazi et al. evaluated the efficacy of titanium mesh cages in the treatment of osteomyelitis in the thoracolumbar vertebrae [5]. Their clinical results showed that average increase in kyphosis of $10 \pm 6°$ corresponding to 4 ± 4 mm loss in the height of the anterior construct. From the implant design point of view, the severe degrees in kyphosis or subsidence occurred because the thickness of the titanium mesh cage was too thin. In 1986, Harms and Biedermann used internal rings to prevent this problem. They suggested that the use of rings fixed internally at both ends of the titanium mesh cage increased the surface contact between the body cage and vertebrae [11]. Our present results obtained from the Taguchi analysis support this conclusion. Increasing the spike height, the spike diameter, and the number of spike rows or decreasing the inner diameter could increase the contact region between the body cage and the vertebrae. Dietl et al. also stated that a interbody fusion cage with many spikes or a hook device could provide a higher pullout resistance [10]. Although the interbody fusion cages and the body cages have different designs and clinical applications, we obtained the similar outcomes as compared with the interbody fusion cages and agreed with their statement. The results of the Taguchi robust design analysis have proved that increasing the number of spike row can increase the pullout resistance. In addition, a body cage with oblique spikes can also obtain a higher pullout resistance. The results of ANOVA showed that the spike row has the highest contribution and the spike type has the lowest contribution. The reason was that increasing the spike row would largely increase the contact region between the body cage and the vertebrae. However, changing the spike type has little or no effect on the pullout strength, because the contact area of the pyramidal spike type was almost the same as compared with that of the conical spike type.

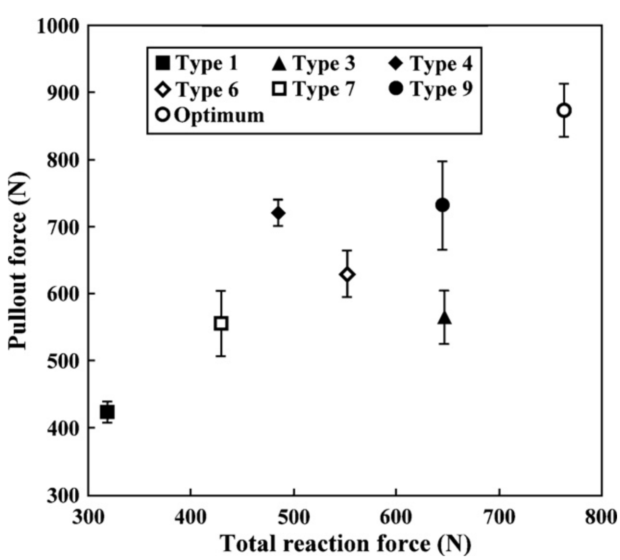

Fig. 6. The correlation study of the body cage.

The clinical implications of a vertebral body replacement cage were to provide initial support and enhance bone fusion. Modifying the design of the body cage can directly improve its clinical performance. However, bone fusion can also increase the stability of the human spine during clinical application. Therefore, the bone fusion condition should also be considered in the body cage design. Knop et al. compared Synex with Harms mesh cage in compression tests. Here human cadaveric specimens of intact vertebrae were used to measure the compression strength of the vertebral body endplate in uniaxial loading. They found that the mean ultimate compression force of Synex is higher than that of Harms mesh cage [1]. According to the geometry of these two design body cages, Synex had a smaller inner diameter (larger contact region) than Harms mesh cage. According to our results, although Synex could provide a higher mechanical strength, the stability of the human spine would be decreased in a situation with bone fusion. Rohlmann et al. developed a three-dimensional finite element model of the lumbar spine with a vertebral body replacement at L3 to discuss the different elastic modulus of fused bone. This paper concluded that bone grafts should be used whenever possible [13]. In this study, the total reaction force of the body cage in a situation with bone fusion has obviously increased by 26% on the average as compared with that in a situation without bone fusion. This implied that this body cage was designed not only considering the geometry and dimensions of the spike but also the fusion condition. Therefore, it has been shown that by merely improving the mechanical performance of the body cage alone, the fusion ability might be compromised. Likewise, the reverse is also true. As a result, the mechanical performance and the fusion ability need to be considered simultaneously for designing a new body cage in the future. The better design combinations of the body cage were obtained after the parametric analysis by Taguchi methods. According to the literature, Knöller et al. conducted an in vitro biomechanical study to evaluate the stability of different types of spinal instruments and to discuss the relationship between the performances of different instrumentation and the bone mineral density. The results showed that a single ventral instrumentation can provide sufficient rigidity in a situation with a high bone mineral density and a combined dorsoventral instrumentation can provide sufficient rigidity even with poor bone density [24]. Therefore, when using the body cage to treat spinal diseases, some additional instrumentation, such as a side plate, should be used in addition to the special design of the body cage, especially for a patient with osteoporotic bones.

Other than the geometry and dimension of the spike design, the feasibility of the surgical implantation was another important issue for the design. For instance, a body cage with higher spikes could increase the pullout strength, but the increased length of the body cage would need a larger space between the vertebrae to implant the body cage. This might cause intraoperative soft tissue injuries, especially vascular injury, and need larger wounds after the orthopaedic surgery. A special body cage with an expandable design had been invented. This kind of design could eliminate this surgical problem. Therefore, an ideal body cage design should also consider these different aspects on a case-by-case basis.

In the mechanical tests, the total reaction force and pullout force of the optimum body cage was superior to that of six types of the body cages. This implied that the Taguchi method could provide a reliable combination of the body cage. Furthermore, in the results of the correlation study, the good relationship between finite element analyses and mechanical tests was found with a correlation coefficient of 0.802. It meant that the finite element models could be used to predict the relatively reliable results of the experiments. In the future study, this finite element model could also be applied for developing a newly body cage.

This research had potential limitations. First, the material properties of the bone were assumed to be homogeneous, isotropic, and linear elastic. This might affect the applicability of the finite element models. Second, Taguchi methods just provide the discrete value of each design variable and rough out the optimum design of the body cage. Third, this study only considers the pullout strength of the body cage. However, the subsidence and pullout strength of the body cage should be considered simultaneously for designing a body cage. Fourth, both bone cuffs of the finite element models were assumed to be parallel and the bony endplates were removed. This might affect the feasibility of the finite element models and the results of the experimental tests.

5. Conclusions

From the results of ANOVA, the spike row (57.01%), spike oblique (12.40%), and spike height (9.31%) were important factors in the situation without bone fusion and the spike row (45.69%), spike height (17.06%), and inner diameter (12.44%) were significant factors in the situation with bone fusion. Based on the S/N ratio plots, the optimum combination of the body cage design in a situation without bone fusion was $ST_1SH_3SD_3SO_3SR_3ID_1$ (the pyramidal spike type, a spike height of 2 mm, a spike diameter of 2.2 mm, an oblique geometry, 11 rows per 28 mm, and an inner diameter of 10 mm), and in the situation with bone fusion it was $ST_2SH_3SD_3SO_3SR_3ID_3$ (the conical spike type, a spike height of 2 mm, a spike diameter of 2.2 mm, an oblique geometry, 11 rows per 28 mm, and an inner diameter of 20 mm). The FEM-based Taguchi methods have effectively decreased the time and effort required for evaluating the design factors of implants and have fairly assessed the contribution of each design factor. The presence of bone fusion and the other additional spinal instrumentation should also be considered during a vertebral body replacement, even when the body cage has a sufficient mechanical strength. The finite element models developed in this study could be used to predict the pullout force of the body cages.

Conflict of interest

None.

References

[1] Knop C, Lange U, Bastian L, Oeser M, Blauth M. Biomechanical compression tests with a new implant for thoracolumbar vertebral body replacement. Eur Spine J 2001;10:30–7.
[2] Pflugmacher R, Schleicher P, Schaefer J, Scholz M, Ludwig K, Khodadadyan-Klostermann C, et al. Biomechanical comparison of expandable cages for vertebral body replacement in the thoracolumbar spine. Spine 2004;29:1413–9.
[3] Vahldiek MJ, Panjabi MM. Stability potential of spinal instrumentations in tumor vertebral body replacement surgery. Spine 1998;23:543–50.
[4] Dvorak MF, Kwon BK, Fisher CG, Eiserloh HL, Boyd M, Wing PC. Effectiveness of titanium mesh cylindrical cages in anterior column reconstruction after thoracic and lumbar vertebral body resection. Spine 2003;28(9):902–8.
[5] Fayazi AH, Ludwig SC, Dabbah M, Butler RB, Gelb DE. Preliminary results of staged anterior debridement and reconstruction using titanium mesh cages in the treatment of thoracolumbar vertebral osteomyelitis. Spine J 2004;4:388–96.
[6] Grant JP, Oxland TR, Dvorak MF, Fisher CG. The effects of bone density and disc degeneration on the structural property distributions in the lower lumbar vertebral endplates. J Orthop Res 2002;20:1115–20.
[7] Jost B, Cripton PA, Lund T, Oxland TR, Lippuner K, Jaeger P, et al. Compressive strength of interbody cages in the lumbar spine: the effect of cage shape, posterior instrumentation and bone density. Eur Spine J 1998;7(2):132–41.
[8] Lim TH, Kwon H, Jeon CH, Kim JG, Sokolowski M, Natarajan R, et al. Effect of endplate conditions and bone mineral density on the

compressive strength of the graft–endplate interface in anterior cervical spine fusion. Spine 2001;26(8):951–6.
[9] Steffen T, Tsantrizos A, Aebi M. Effect of implant design and endplate preparation on the compressive strength of interbody fusion constructs. Spine 2000;25(9):1077–84.
[10] Dietl RHJ, Krammer M, Kettler A, Wilke HJ, Claes L, Lumenta CB. Pullout test with three lumbar interbody fusion cages. Spine 2002;27(10):1029–36.
[11] Grob D, Daehn S, Mannion AF. Titanium mesh cages (TMC) in spine surgery. Eur Spine J 2005;14(3):211–21.
[12] Thongtyrangan I, Balabhadra R, Le H, Park J, Kim DH. Vertebral body replacement with and expandable cage for reconstruction after spinal tumor resection. Neurosurg Focus 2003;15(5):1–6.
[13] Rohlmann A, Zander T, Bergmann G. Effects of fusion-bone stiffness on the mechanical behavior of the lumbar spine after vertebral body replacement. Clin Biomech 2006;21:221–7.
[14] Chao CK, Hsu CC, Wang JL, Lin J. Increasing bending strength of tibial locking screws: mechanical tests and finite element analyses. Clin Biomech 2007;22:59–66.
[15] Dar FH, Aspden RM. A finite element model of an idealized diarthrodial joint to investigate the effects of variation in the mechanical properties of the tissues. Proc Inst Mech Eng H: J Eng Med 2003;217(5):341–8.
[16] Hou SM, Hsu CC, Wang JL, Chao CK, Lin J. Mechanical tests and finite element models for bone holding power of tibial locking screws. Clin Biomech 2004;19:738–45.
[17] Hsu CC, Chao CK, Wang JL, Lin J. Multiobjective optimization of tibial locking screws design using a genetic algorithm: evaluation of mechanical performance. J Orthop Res 2006;24(5):908–16.
[18] Lin CL, Chang SH, Chang WJ, Kuo YC. Factorial analysis of variables influencing mechanical characteristics of a single tooth implant placed in the maxilla using finite element analysis and the statistics-based Taguchi method. Eur J Oral Sci 2007;115(5): 408–16.
[19] Mburu G, Aspden RM, Hutchison JD. Optimising the configuration of cement keyholes for acetabular fixation in total hip replacement using Taguchi experimental design. Proc Inst Mech Eng H: J Eng Med 1999;213:485–92.
[20] Singer G, Ebramzadeh E, Jones NF, Meals R. Use of the Taguchi method for biomechanical comparison of flexor-tendon-repair techniques to allow immediate active flexion. A new method of analysis and optimization of technique to improve the quality of the repair. J Bone Joint Surg Am 1998;80(10):1498–506.
[21] Yao J, Funkenbusch PD, Snibbe J, Maloney M, Lerner AL. Sensitivities of medial meniscal motion and deformation to material properties of articular cartilage, meniscus and meniscal attachments using design of experiments methods. J Biomech Eng 2006;128(3): 399–408.
[22] Dar FH, Meakin JR, Aspden RM. Statistical methods in finite element analysis. J Biomech 2002;35:1155–61.
[23] Fowlkes WY, Creveling CM. Engineering methods for robust production design using Taguchi method in technology and product development. Reading: Addison Wesley; 1995.
[24] Knöller SM, Meyer G, Eckhardt C, Lill CA, Schneider E, Linke B. Range of motion in reconstruction situations following corpectomy in the lumbar spine: a question of bone mineral density? Spine 2005;30(9):E229–35.